






Exponentially faster preparation of quantum dimers via driven-dissipative stabilization

Kian Hwee Lim ^{1,*} Wai-Keong Mok ^{2,†} Jia-Bin You ³ Jian Feng Kong ³ and Davit Aghamalyan ³

¹Centre for Quantum Technologies, National University of Singapore, 3 Science Drive 2, Singapore 117543

²Institute for Quantum Information and Matter,

California Institute of Technology, Pasadena, CA 91125, USA

³Institute of High Performance Computing, A*STAR (Agency for Science, Technology and Research), 1 Fusionopolis Way, #16-16 Connexis, Singapore 138632

We propose a novel rapid, high-fidelity, and noise-resistant scheme to generate many-body entanglement between multiple qubits stabilized by dissipation into a 1D bath. Using a carefully designed time-dependent drive, our scheme achieves a provably exponential speedup over state-of-the-art dissipative stabilization schemes in 1D baths, which require a timescale that diverges as the target fidelity approaches unity and scales exponentially with the number of qubits. To prepare quantum dimer pairs, our scheme only requires local 2-qubit control Hamiltonians, with a protocol time that is independent of system size. This provides a scalable and robust protocol for generating a large number of entangled dimer pairs on-demand, serving as a fundamental resource for many quantum metrology and quantum information processing tasks.

Introduction.— Entangled quantum states are essential for quantum computation [1] and metrology [2], which demand their high fidelity generation in a way that is resilient to noise and dissipation. Dissipation, once seen as detrimental, is now explored as a resource for entanglement generation [3]. However, despite a plethora of theoretical proposals and experimental realizations for generating entangled states with cavity quantum electrodynamics (QED) systems [3–7], ion traps [8–10], Rydberg atoms [11–14], colour centers [15–18], circuit QED [19, 20], optical lattices and spin chains [21–25], limitations persist in either the speed of state generation, entanglement fidelity or the aforementioned robustness to noise and dissipation. For instance, the dissipative entanglement generation schemes based on Ref. [3] rely on perturbative expansions in the system’s driving strengths, which fundamentally limits the speed of entanglement generation.

It was also shown in [26, 27] that when multiple locally-driven system qubits are coupled to a chiral 1D bath (which could either be a waveguide or a spin chain), one can obtain many-body entangled states stabilized by the dissipation into the 1D bath. In this theoretical scheme, no perturbative expansions in the system’s driving strengths are required, which circumvents the aforementioned speed limit. An atomic implementation of this scheme on cold quantum gases was proposed in [21], and experimentally implemented recently on superconducting qubits [28].

However, as we will demonstrate in this manuscript, time-independent many-body entanglement generation schemes using engineered dissipation as proposed in [21, 26, 27] require a timescale that diverges as the target fidelity approaches unity, leading to an inevitable trade-off between fidelity and speed. Furthermore, for existing steady state schemes including [29], the protocol time scales exponentially with the number of qubits. This presents a severe limitation for scaling up to many

qubits, especially in the presence of noise. We propose a new scalable protocol based on carefully designed time-dependent driving to generate many-body entanglement in 1D systems in a fast, high-fidelity and noise-robust manner. To the best of our knowledge, our scheme is the only one that fulfils this trifecta.

An important application of our scheme is in preparing a large number of quantum dimer pairs on-demand, which are valuable resource states for various quantum technologies such as quantum metrology [29, 30] and quantum information processing. Our scheme achieves a high-fidelity preparation using only local 2-qubit control Hamiltonians, rendering it feasible to current experimental capabilities. Crucially, our protocol time is independent of the number of qubits, thereby exponentially faster than the previously proposed schemes [21, 26, 27, 29]. We perform a systematic study of robustness of our scheme against various sources of noise and decoherence. We show that in the presence of any amount of spontaneous decay outside of the 1D bath, previous time-independent schemes eventually fail for a sufficiently large number of qubits due to the exponentially long timescales required. On the contrary, our scheme is robust against such losses for any number of qubits.

Many-body entangled dark states of 1D systems.— In waveguide QED, one often considers the case where there are N qubits coupled to a 1D bath [27, 31]. The 1D bath serves firstly as a decay channel for the system qubit excitations, and secondly to mediate long-distance coherent interactions between the system qubits. With reference to Fig. 1, under the Born-Markov and rotating wave approximations, by tracing out the 1D bath, we obtain the following Hamiltonian (setting $\hbar = 1$) for the N system qubits

$$H_S = - \sum_{i=1}^N \delta_i \sigma_i^\dagger \sigma_i + H_{\text{drive}}(t) + \sum_{j < k} (H_C)_{jk} \quad (1)$$

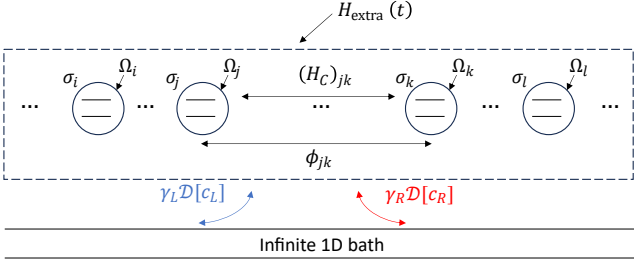


FIG. 1. Schematic for the setup described by Eq. (1) and Eq. (2). N qubits are coupled to a waveguide as per [26] or to a 1D spin chain with a synthetic gauge field as per [27]. Here, σ_j is the lowering operator for j th system qubit that is driven with an external local drive Ω_j . ϕ_{jk} describes the phase picked up by the bath excitation as it travels between the j th and k th qubit along the infinite 1D bath, which affects the bath-mediated chiral interaction between the j th and k th qubit. H_{extra} is the extra external field in our scheme which we will introduce later. All the qubits decay collectively into the 1D bath through collective jump operators c_L (left-going modes) and c_R (right-going modes) with decay rates γ_L and γ_R respectively.

where $(H_C)_{jk} = \frac{i}{2}(\gamma_R e^{-i\phi_{jk}} - \gamma_L e^{i\phi_{jk}})\sigma_j^\dagger \sigma_k + \text{H.c}$ describes the coherent interaction mediated by the 1D bath between the j th and k th system qubits, $H_{\text{drive}}(t) = \sum_{i=1}^N (\Omega_i(t)/2)\sigma_i + \text{H.c}$ describes the local driving on the qubits with Rabi frequency $\Omega_i(t)$, δ_i describe the detuning between the i th qubit and the carrier frequency of the 1D bath. The dissipation of the system into the 1D bath is described by a master equation for the N system qubits [26, 27]

$$\dot{\rho} = -i[H_S, \rho] + \gamma_L \mathcal{D}[c_L]\rho + \gamma_R \mathcal{D}[c_R]\rho. \quad (2)$$

Here, $\mathcal{D}[c_{L(R)}]\rho = c_{L(R)}\rho c_{L(R)}^\dagger - \{c_{L(R)}^\dagger c_{L(R)}, \rho\}/2$ describes the leftward (rightward) dissipation of the system qubits into the bath, where $c_L = \sum_{j=1}^N e^{i\phi_j} \sigma_j$, $c_R = \sum_{j=1}^N e^{-i\phi_j} \sigma_j$ are the collective jump operators. The system is chiral if $\gamma_L \neq \gamma_R$, physically manifesting as an asymmetric emission into the bath. While entanglement generation schemes which operate in the transient regime for these 1D systems have been proposed [32, 33], a higher fidelity that is also stabilized by the dissipation into the bath can be attained in the steady state [26, 29]. In particular, it was shown [26] that when $\phi_{jk} \bmod 2\pi = 0$, together with certain conditions on δ_i (or in the chiral case $\gamma_L \neq \gamma_R$) with homogeneous time-independent driving $\Omega_i(t) = \Omega$, it is possible to obtain the following multipartite entangled dark steady state

for even N

$$\rho_{ss} = |\Phi\rangle\langle\Phi|, \quad \text{where } |\Phi\rangle = \prod_{q=1}^{N_m} |M_q\rangle \quad (3a)$$

$$|M_q\rangle = a^{(0)}|g\rangle^{\otimes M_q} + \sum_{j_1 < j_2} a_{j_1, j_2}^{(1)} |S\rangle_{j_1 j_2} |g\rangle^{\otimes M_q - 2} + \dots + \sum a_{j_1, \dots, j_{M_q/2}}^{(M_q/2)} |S\rangle_{j_1 j_2} \dots |S\rangle_{j_{M_q-1} j_{M_q}}. \quad (3b)$$

We define $|S\rangle_{ij} = (|e\rangle_i |g\rangle_j - |g\rangle_i |e\rangle_j)/\sqrt{2}$ as a singlet state (or a dimer pair) between qubits i and j . $|\Phi\rangle$ is a product of N_m adjacent multimers $|M_q\rangle$, and each $|M_q\rangle$ is an entangled state over M_q qubits as defined in Eq. (3b), where M_q is an even integer. Note that the summation in the last line of Eq. (3b) runs over all different pairings of qubits $\{(j_1, j_2), \dots, (j_{M_q-1}, j_{M_q})\}$ with $j_k < j_{k+1}$. It can also be shown that $a^{(i)} \propto |\Omega|^{-M_q/2+i}$ [26]. In the above equation, of particular interest is the $N_m = 1$, $M_q = N$ case, since that corresponds to the maximal genuine entanglement (across all bipartite cuts of qubits). We also consider $|\Omega| \rightarrow \infty$, since it is the most relevant for metrology [29, 30]. Hence, we shall focus on obtaining the state

$$|\Phi\rangle \propto \sum |S\rangle_{i_1 i_2} |S\rangle_{i_3 i_4} \dots |S\rangle_{i_{N-1} i_N} \quad (4)$$

where the summation in Eq. (4) runs over different pairings of qubits $\{(i_1, i_2), (i_3, i_4), \dots, (i_{N-1}, i_N)\}$ where $i_j < i_{j+1}$. By a suitable detuning pattern, it is also possible to obtain the special case where there is only one term in the sum, such that the system forms dimerised pairs of qubits in the steady state. However, we will now show that such schemes require a prohibitively long time to generate high-fidelity, many-body entanglement.

Divergent timescale of preparing entangled dark states.— As mentioned in [26], the timescale required to form one dimer pair from $N = 2$ qubits diverges as the target fidelity approaches one. This can also be seen by analysing the Liouvillian gap [34, 35] (see Supplemental Material [36]), but is analytically challenging for large N . By using a recently developed general framework for analysing quantum speed limits in dissipative state preparation [37], we derive a lower bound on the time T required to generate the state in Eq. (3) for any system size N (see Supplementary Material [36] for a derivation)

$$T \geq T_{\text{QSL}} \propto \prod_{q=1}^{N_m} |\Omega|^{M_q/2} = |\Omega|^{N/2} \sim \left(\frac{1}{1-F}\right)^{N/4}. \quad (5)$$

The preparation time diverges as $|\Omega| \rightarrow \infty$, or equivalently as the fidelity F to the target state in Eq. (4) approaches unity. Crucially, for any fixed target fidelity F , the preparation time scales exponentially with the number of qubits N .

In the presence of *any* spontaneous decay rate Γ_f outside of the 1D bath, the time-independent scheme would

fail when the preparation time required exceeds $\sim 1/\Gamma_f$. From Eq. (5), we can estimate that the time-independent scheme fails for $N \gtrsim \log(\Gamma/\Gamma_f)$, where $\Gamma = \gamma_L + \gamma_R$ is the total decay rate into the 1D bath. This can be interpreted as a fundamental trade-off between fidelity and speed, and highlights a severe limitation to the scalability of such schemes. We now propose an exponentially faster scheme that circumvents all these problems while retaining the robustness from dissipative stabilization.

Exponentially faster scheme for many-body entanglement generation. — Our scheme deviates from the previously proposed time-independent schemes in two important aspects. Firstly, instead of a time-independent homogeneous drive $\Omega_j = \Omega$, we consider $\Omega_j = \Omega(t)$ such that $\Omega(0) = 0$ and $\Omega(t)$ is any non-decreasing real-valued function of t . Secondly, all the detunings δ_j are zero, even at zero chirality. In this case, with $\phi_{jk} \bmod 2\pi = 0$, in the master equation Eq. (2), we have $\gamma_L \mathcal{D}[c_L] + \gamma_R \mathcal{D}[c_R] = \Gamma \mathcal{D}[c]\rho$ where $c = \sum_{j=1}^N \sigma_j$, $\Gamma = \gamma_L + \gamma_R$, and $(H_C)_{jk} = (i\Delta\gamma/2)(\sigma_j^\dagger \sigma_k - \sigma_j \sigma_k^\dagger)$ where $\Delta\gamma = \gamma_R - \gamma_L$. We define the total coherent interaction term as $H(t) \equiv H_C + H_{\text{drive}}(t)$, where $H_C = \sum_{j < k} (H_C)_{jk}$.

Our scheme begins by choosing a target state $|\Phi\rangle$ of the form in Eq. (4), where in the summation, we have the freedom to choose which different pairings of qubits to sum over. Let $\theta(\Omega(t))$ be a function where $\theta(\Omega(t) = 0) = 0$, $\theta(\Omega(t) = \infty) = \pi/2$. For example, $\theta(\Omega(t))$ could be

$$\theta(\Omega(t)) = \frac{\pi}{2}(1 - e^{-k\Omega(t)/\Gamma}), \quad k > 0, \quad (6)$$

though many other examples exist. The main idea is that both the initial state $|g\rangle^{\otimes N}$ and the target state $|\Phi\rangle$ at $\Omega(t) \rightarrow \infty$ are instantaneous steady states, which means that if we can generate the unitary evolution $U(\theta(\Omega))|g\rangle^{\otimes N} = \cos(\theta(\Omega))|g\rangle^{\otimes N} - i\sin(\theta(\Omega))|\Phi\rangle$, then $\Omega \rightarrow \infty$ gives us $U(\theta(\Omega))|g\rangle^{\otimes N} = |\Phi\rangle$. In practice, we do not require $\Omega(t) \rightarrow \infty$, since at large $\Omega(t)$ such that $\theta(\Omega) = \pi/2 - \epsilon$, $U(\theta)$ already prepares a state $|\psi(\theta)\rangle \equiv U(\theta)|g \dots g\rangle$ with a fidelity of $F = |\langle\psi(\theta)|\Phi\rangle|^2 = \cos^2(\epsilon) \approx 1 - \epsilon^2$ to $|\Phi\rangle$. Hence, by a judicious choice of $\theta(\Omega(t))$ and $\Omega(t)$, we can achieve a state $|\psi(\theta)\rangle$ that has very high fidelity to $|\Phi\rangle$ at times much shorter than the dissipation timescale Γ^{-1} . Using Eq. (6) as an example, for $k\Omega(t)/\Gamma \approx 4$, we have $F \approx 0.999$. After preparing $|\psi(\theta)\rangle$ at a short time t_f , we keep $\Omega(t > t_f)$ constant. This causes the state to relax towards the steady state close to $|\Phi\rangle$. Thus, our scheme works with a high fidelity even for a finite Ω , rendering its practicality. In short, our scheme moves along a trajectory within the decoherence-free subspace spanned by $|g\rangle^{\otimes N}$ and $|\Phi\rangle$ and is thus dissipation-stabilized.

To construct $U(\theta)$, we first define $X \equiv |g\rangle^{\otimes N}\langle\Phi| + |\Phi\rangle\langle g\rangle^{\otimes N}$ and then see that $U(\theta) = \exp\left(-i \int_0^t (\partial_t \theta) X dt'\right)$ which means that the de-

sired $U(\theta)$ can be generated by the Hamiltonian $H_u(t) = (\partial_t \theta)X$. Thus, we simply need to add an extra time-dependent control field $H_{\text{extra}}(t) \approx H_u(t)$ to our system Hamiltonian $H(t)$. This extra time-dependent control field would only need to be switched on from $t = 0$ to $t = t_f$ for some finite t_f to generate $U(\theta)$, after which the time-dependence can be switched off and $\Omega(t)$ held constant. One might be concerned about spurious effects from the coherent interactions mediated by the 1D bath. While this can be entirely mitigated in $H_{\text{extra}}(t)$, we find that it is unnecessary. The validity of the approximation $H_{\text{extra}}(t) \approx H_u(t)$ is discussed in detail in the Supplemental Material [36], but here we note the following two points. Firstly, the approximation is better for a smaller $\Delta\gamma$, with the best case being zero chirality ($\Delta\gamma = 0$). This is actually an advantage when compared to [26] which requires $\Delta\gamma \neq 0$ when all the detunings δ_i are zero. Secondly, by choosing $\partial_t \theta$ to be as large as possible, we can perform the transformation $|g\rangle^{\otimes N} \rightarrow |\psi(\theta)\rangle \approx |\Phi\rangle$ in this decoherence-free subspace arbitrarily quickly, which also improves the approximation $H_{\text{extra}}(t) \approx H_u(t)$.

We stress that while this protocol looks similar to the idea of counterdiabatic driving in decoherence-free subspaces [38–40] due to the presence of an additional time-dependent control Hamiltonian, it is different in many ways. Unlike counterdiabatic driving, the state $|\psi(\theta)\rangle$ does not need to be an instantaneous eigenstate of $H(t)$. In fact, moving along the adiabatic trajectory in the Hilbert space as proposed in [26] requires $\Delta\gamma \neq 0$, whereas our scheme allows for $\Delta\gamma = 0$. Thus, our scheme is fundamentally different from the various shortcut-to-adiabaticity schemes [41]. In our computation of the extra driving field $H_{\text{extra}}(t)$, unlike the various counterdiabatic driving schemes, we do not require all the instantaneous eigenstates of $H(t)$. This is highly advantageous in many situations where an exact diagonalization of $H(t)$ is difficult, such as for large N . More details about the differences between our proposed scheme and counterdiabatic driving can be found in the Supplemental Material [36].

In our scheme, the key part is implementing the X operator, which can be experimentally difficult for certain target states $|\Phi\rangle$ due to the many-body interactions required to generate X . An example for $N = 6$ qubits is shown in the Supplemental Material [36]. However, when $|\Phi\rangle$ describes the state of $N/2$ dimerised pairs, applying the above formalism gives us $U(\theta) = U_{i_1 i_2}(\theta)U_{i_3 i_4}(\theta) \dots U_{i_{N-1} i_N}(\theta)$ where $U_{i_k i_{k+1}}(\theta) = \cos(\theta)\mathbb{1} - i\sin(\theta)X_{i_k i_{k+1}}$, and $X_{i_k i_{k+1}} = |gg\rangle\langle S|_{i_k i_{k+1}} + |S\rangle\langle gg|_{i_k i_{k+1}}$ is a two-body interaction term between qubits i_k and i_{k+1} . $U(\theta)$ can then be generated by the Hamiltonian $H_u(t) = (\partial_t \theta)X$ where $X = X_{i_1 i_2} + X_{i_2 i_3} + \dots + X_{i_{N-1} i_N}$. Finally, we have $H_{\text{extra}}(t) \approx H_u(t)$, which means that it suffices for the engineered control Hamiltonian to be 2-qubit interac-

tions. Explicitly, for geometrically local dimer pairs, we have $H_{\text{extra}}(t) \approx \sum_{k \text{ odd}} V_{k,k+1}$ where $V_{k,k+1} = (\partial_t \theta) \left(\frac{1}{2}(\sigma_k^x - \sigma_{k+1}^x) + \frac{1}{2}(\sigma_k^z \sigma_{k+1}^z - \sigma_k^y \sigma_{k+1}^y) \right)$. Since the control Hamiltonian is local and can be applied in parallel, our protocol time is independent of N , which is exponentially faster than state-of-the-art time-independent schemes [26, 29] while still benefiting from dissipative stabilization.

Fig. 2 shows the results of numerical experiments comparing our scheme against previous proposals. We also benchmark our scheme against an adiabatic scheme. As can be seen, at short timescales $\Gamma t \ll 1$, our scheme achieves concurrence ≈ 1 for the case where $\Delta\gamma = 0$ and concurrence ≈ 0.97 for the case where $\Delta\gamma/\Gamma = 1$. On the other hand, the adiabatic scheme fails at timescales $\Gamma t \ll 1$ as the driving strength is modulated too quickly, violating the adiabatic condition for open quantum systems [42]. This is corroborated by a sharp drop in purity between $0 < t < t_f$. After $t > t_f$ where the driving strengths become fixed, the adiabatic and the time-independent schemes become very similar. Our scheme is scalable and can be used to generate many dimer pairs simultaneously.

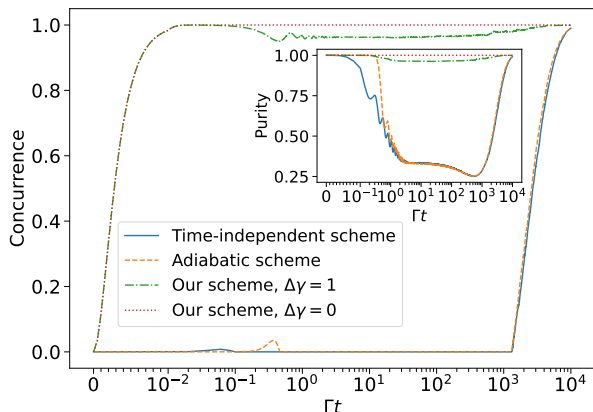


FIG. 2. The case of $N = 8$ qubits forming $N/2 = 4$ geometrically local dimer pairs $\{(1, 2), (3, 4), (5, 6), (7, 8)\}$. Since all dimer pairs are treated equally, we plot the concurrence [43] and the purity (in the inset) between the qubits (1, 2) for various entanglement generation schemes mentioned in the main text. For our scheme, we use Eq. (6) with $k = 10$. For both our scheme and the adiabatic scheme, we use the linear ramp function $\Omega(t)/\Gamma = m\Gamma t\Theta(t_f - t) + m\Gamma t_f\Theta(t - t_f)$ saturating at $t = t_f$, where $\Theta(t)$ is the Heaviside step function with $\Theta(0) = 1/2$, and with $m = 25$, $t_f = \Gamma^{-1}$, whereas for the time-independent scheme, we have $\Omega/\Gamma = 25$. For both the adiabatic scheme and the time-independent scheme, we have $\Delta\gamma/\Gamma = 1$, and also the appropriate detuning conditions as proposed in [26]. The adiabatic schemes and the time-independent schemes are very similar after $t > t_f$ because the driving strengths $\Omega(t)$ become fixed after $t > t_f$. Clearly, only our scheme succeeds at short timescales $\Gamma t \ll 1$.

Robustness analysis. — We consider the robustness of our scheme to two types of noise which arise from imperfect control. Let $\xi_1(t)$ and $\xi_2(t)$ be two independent Gaussian white noise random variables with zero mean and unit variance. A stochastic fluctuation in $H_{\text{drive}}(t)$ can be modelled by making the replacement $H_{\text{drive}}(t) \rightarrow (1 + \eta_1 \xi_1(t))H_{\text{drive}}(t)$. Similarly, a stochastic fluctuation in $H_{\text{extra}}(t)$ can be modelled by making the replacement $H_{\text{extra}}(t) \rightarrow (1 + \eta_2 \xi_2(t))H_{\text{extra}}(t)$. Following [41, 44], we average over the white noise random variables using Novikov's theorem for white noise [45] to obtain the following modified master equation $\dot{\rho} = -i[H_{\text{drive}}(t) + H_{\text{extra}}(t), \rho] + \Gamma \mathcal{D}[c]\rho + \eta_1^2 \mathcal{D}[H_{\text{drive}}(t)]\rho + \eta_2^2 \mathcal{D}[H_{\text{extra}}(t)]\rho$. Using $\theta(\Omega(t))$ from Eq. (6) with $k = 10$, and $\Omega(t) = mt$, $m > 0$, we numerically study the effect of η_i separately in Fig. 3 for the $\Delta\gamma = 0$ case. Our scheme is robust against noise in H_{drive} regardless of how fast $\Omega(t)$ is increased. The reason is that our scheme works as long as $\Omega(t)/\Gamma \gg 1$ at large t , such that the fluctuations $\Omega(t)/\Gamma$ are insignificant. On the other hand, when dealing with noise in $H_{\text{extra}}(t)$, there is a tradeoff between the amount of noise present η_2 and the maximum m allowed such that the concurrence remains high, which can be explained by the adiabatic theorem for open quantum systems [42].

Another common source of noise is spontaneous decay outside of the 1D bath. As discussed earlier, the time-independent schemes fail completely for $N \gtrsim \log(\Gamma/\Gamma_f)$ where Γ_f is the spontaneous decay rate, due to the exponentially long timescales needed. In contrast, our scheme is able to generate quantum dimers with high concurrence for any N on the relevant system timescale Γ^{-1} , as long as $\Gamma_f/\Gamma \ll 1$, which is achievable in current experiments (see Supplementary Materials [36] for more details).

Discussion. — We present a new scheme for rapid, high fidelity generation of many-body entanglement for qubits coupled to a 1D bath, which is also robust to noise. Our scheme is exponentially faster than previously proposed time-independent schemes in [21, 26, 27, 29], and does not require chirality or specific detuning patterns on the qubits, which makes it more convenient for experimental implementation. Our scheme avoids the usual drawbacks of dissipative state preparation in open systems such as the use of time-dependent dissipators or potentially unphysical dynamics [39]. Remarkably, to generate geometrically local dimer pairs, we only require 2-qubit control Hamiltonians $H_{\text{extra}}(t)$, which can be experimentally implemented in superconducting qubits [46–49]. Non-local interactions between the dimers are suppressed by destructive interference.

Furthermore, recent experiments using superconducting qubits work with free space spontaneous emission and dephasing decay rates of $\Gamma_f/2\pi \approx 15$ kHz and $K_\phi/2\pi \approx 100$ KHz [50]. Considering a typical decay rate of a single qubit into a waveguide $\Gamma/2\pi \approx 15$ MHz, from Fig. 2, it is clear that our scheme is faster than the superconduct-

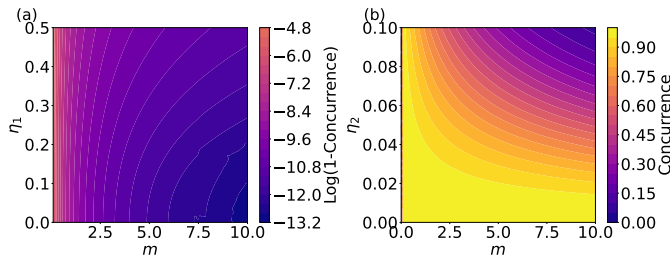


FIG. 3. Analysis of the robustness of our scheme against noise. Here, we use Eq. (6) for $\theta(\Omega(t))$ with $k = 10$ and $\Omega(t) = mt$, and we consider the case where $\Delta\gamma = 0$ in generating 4 dimerised pairs from $N = 8$ qubits. Since the concurrences of all the dimers are the same, we use the concurrence of a dimer pair at the steady state to characterise the entanglement generated. In (a), since the values of concurrence C of the final state obtained are all close to 1, we plot $\log(1 - C)$ against η_1 and m while assuming $\eta_2 = 0$, and in (b), we plot the concurrence of the final state obtained as a function of η_2 and m but with assuming $\eta_1 = 0$. From (a), since the values of the concurrence C are all close to 1, we see that our scheme is relatively insensitive to fluctuations in the driving strength $\Omega(t)$ regardless of how fast we increase the driving, though there is still some trade-off. From (b), we see that there is a trade-off between the amount of noise allowed and the rate m at which we can increase the driving strength Ω .

ing qubit decoherence times. Since the time-independent scheme has been recently demonstrated experimentally with superconducting qubits [28], it is a promising platform to realize our exponentially faster protocol. As potential future work, it is worth exploring the possibility of approximating the many-body interaction terms in our general scheme using local driving terms, following the formalism developed in [51, 52] for counterdiabatic driving.

The IHPC A*STAR Team acknowledges support from the National Research Foundation Singapore (NRF2021-QEP2-02-P01), A*STAR Career Development Award (C210112010), and A*STAR (C230917003, C230917007). K.H.L is grateful to the National Research Foundation and the Ministry of Education, Singapore for financial support. The Institute for Quantum Information and Matter is an NSF Physics Frontiers Center. We thank William Chen, Leong-Chuan Kwek, Parth Shah, Richard Tsai, Sai Vinjanampathy and Frank Yang for helpful discussions.

* Equal contribution; kianhwee.lim@u.nus.edu

† Equal contribution

- [1] M. A. Nielsen and I. Chuang, Quantum computation and quantum information (2002).
- [2] V. Giovannetti, S. Lloyd, and L. Maccone, *Nature photonics* **5**, 222 (2011).
- [3] M. J. Kastoryano, F. Reiter, and A. S. Sørensen, *Physical*

- review letters* **106**, 090502 (2011).
- [4] F. Reiter, M. J. Kastoryano, and A. S. Sørensen, *New Journal of Physics* **14**, 053022 (2012).
- [5] R. Sweke, I. Sinayskiy, and F. Petruccione, *Physical Review A* **87**, 042323 (2013).
- [6] S.-L. Su, X.-Q. Shao, H.-F. Wang, and S. Zhang, *Physical Review A* **90**, 054302 (2014).
- [7] L.-T. Shen, X.-Y. Chen, Z.-B. Yang, H.-Z. Wu, and S.-B. Zheng, *Physical Review A* **84**, 064302 (2011).
- [8] Y. Lin, J. Gaebler, F. Reiter, T. R. Tan, R. Bowler, A. Sørensen, D. Leibfried, and D. J. Wineland, *Nature* **504**, 415 (2013).
- [9] D. C. Cole, J. J. Wu, S. D. Erickson, P.-Y. Hou, A. C. Wilson, D. Leibfried, and F. Reiter, *New Journal of Physics* **23**, 073001 (2021).
- [10] D. C. Cole, S. D. Erickson, G. Zarantonello, K. P. Horn, P.-Y. Hou, J. J. Wu, D. H. Slichter, F. Reiter, C. P. Koch, and D. Leibfried, *Physical Review Letters* **128**, 080502 (2022).
- [11] R. Li, D. Yu, S.-L. Su, and J. Qian, *Physical Review A* **101**, 042328 (2020).
- [12] X.-Q. Shao, J.-B. You, T.-Y. Zheng, C. H. Oh, and S. Zhang, *Phys. Rev. A* **89**, 052313 (2014).
- [13] Y.-H. Chen, Z.-C. Shi, J. Song, Y. Xia, and S.-B. Zheng, *Physical Review A* **97**, 032328 (2018).
- [14] D. D. B. Rao and K. Mølmer, *Phys. Rev. A* **90**, 062319 (2014).
- [15] Y.-F. Qiao, H.-Z. Li, X.-L. Dong, J.-Q. Chen, Y. Zhou, and P.-B. Li, *Physical Review A* **101**, 042313 (2020).
- [16] Z. Jin, S. L. Su, and S. Zhang, *Phys. Rev. A* **100**, 052332 (2019).
- [17] D. D. B. Rao, S. Yang, and J. Wrachtrup, *Phys. Rev. A* **95**, 022310 (2017).
- [18] P.-B. Li, S.-Y. Gao, H.-R. Li, S.-L. Ma, and F.-L. Li, *Physical Review A* **85**, 042306 (2012).
- [19] Z. Leghtas, U. Vool, S. Shankar, M. Hatridge, S. M. Girvin, M. H. Devoret, and M. Mirrahimi, *Physical Review A* **88**, 023849 (2013).
- [20] F. Reiter, L. Tornberg, G. Johansson, and A. S. Sørensen, *Physical Review A* **88**, 032317 (2013).
- [21] T. Ramos, H. Pichler, A. J. Daley, and P. Zoller, *Physical review letters* **113**, 237203 (2014).
- [22] G. Kordas, S. Wimberger, and D. Witthaut, *Europhysics Letters* **100**, 30007 (2012).
- [23] T. Botzung, S. Diehl, and M. Müller, *Physical Review B* **104**, 184422 (2021).
- [24] G. Morigi, J. Eschner, C. Cormick, Y. Lin, D. Leibfried, and D. J. Wineland, *Physical Review Letters* **115**, 200502 (2015).
- [25] G. D. de Moraes Neto, V. F. Teizen, V. Montenegro, and E. Vernek, *Phys. Rev. A* **96**, 062313 (2017).
- [26] H. Pichler, T. Ramos, A. J. Daley, and P. Zoller, *Phys. Rev. A* **91**, 042116 (2015).
- [27] T. Ramos, B. Vermersch, P. Hauke, H. Pichler, and P. Zoller, *Phys. Rev. A* **93**, 062104 (2016).
- [28] P. S. Shah, F. Yang, C. Joshi, and M. Mirhosseini, arXiv preprint arXiv:2402.15701 (2024).
- [29] R. Gutiérrez-Jáuregui, A. Asenjo-Garcia, and G. S. Agarwal, *Phys. Rev. Res.* **5**, 013127 (2023).
- [30] P. Groszkowski, M. Koppenhöfer, H.-K. Lau, and A. A. Clerk, *Phys. Rev. X* **12**, 011015 (2022).
- [31] D. Castells-Graells, D. Malz, C. C. Rusconi, and J. I. Cirac, *Phys. Rev. A* **104**, 063707 (2021).
- [32] W.-K. Mok, J.-B. You, L.-C. Kwek, and D. Aghamalyan,

- Physical Review A **101**, 053861 (2020).
- [33] W.-K. Mok, D. Aghamalyan, J.-B. You, T. Haug, W. Zhang, C. E. Png, and L.-C. Kwek, *Physical Review Research* **2**, 013369 (2020).
- [34] V. V. Albert and L. Jiang, *Phys. Rev. A* **89**, 022118 (2014).
- [35] D. Manzano and P. Hurtado, *Advances in Physics* **67**, 1 (2018), <https://doi.org/10.1080/00018732.2018.1519981>.
- [36] See Supplemental Material for (a) Liouvillian gap analysis of timescale for $N = 2$, (b) Derivation of the divergent timescale of preparing entangled dark states (c) Comparison between our scheme and counterdiabatic driving, (d) Approximation of H_{extra} , (e) Effect of single spin spontaneous emission into free space on our protocol (f) Effect of unequal local light-matter coupling (g) $N = 6$ multimers. The Supplemental Material includes Refs. [53], [54], [55].
- [37] J. Liu and H. Nie, *Phys. Rev. A* **107**, 052608 (2023).
- [38] M. V. Berry, *Journal of Physics A: Mathematical and Theoretical* **42**, 365303 (2009).
- [39] G. Vacanti, R. Fazio, S. Montangero, G. M. Palma, M. Paternostro, and V. Vedral, *New Journal of Physics* **16**, 053017 (2014).
- [40] S. L. Wu, X. L. Huang, H. Li, and X. X. Yi, *Phys. Rev. A* **96**, 042104 (2017).
- [41] D. Guéry-Odelin, A. Ruschhaupt, A. Kiely, E. Torrontegui, S. Martínez-Garaot, and J. G. Muga, *Rev. Mod. Phys.* **91**, 045001 (2019).
- [42] L. C. Venuti, T. Albash, D. A. Lidar, and P. Zanardi, *Phys. Rev. A* **93**, 032118 (2016).
- [43] W. K. Wootters, *Quantum Inf. Comput.* **1**, 27 (2001).
- [44] A. Ruschhaupt, X. Chen, D. Alonso, and J. G. Muga, *New Journal of Physics* **14**, 093040 (2012).
- [45] E. A. Novikov, *Sov. Phys. JETP* **20**, 1290 (1965).
- [46] A. Blais, J. Gambetta, A. Wallraff, D. I. Schuster, S. M. Girvin, M. H. Devoret, and R. J. Schoelkopf, *Phys. Rev. A* **75**, 032329 (2007).
- [47] S. Sheldon, E. Magesan, J. M. Chow, and J. M. Gambetta, *Phys. Rev. A* **93**, 060302 (2016).
- [48] B. K. Mitchell, R. K. Naik, A. Morvan, A. Hashim, J. M. Kreikebaum, B. Marinelli, W. Lavrijsen, K. Nowrouzi, D. I. Santiago, and I. Siddiqi, *Phys. Rev. Lett.* **127**, 200502 (2021).
- [49] D.-W. Wang, C. Song, W. Feng, H. Cai, D. Xu, H. Deng, H. Li, D. Zheng, X. Zhu, H. Wang, *et al.*, *Nature Physics* **15**, 382 (2019).
- [50] M. Zanner, T. Orell, C. M. Schneider, R. Albert, S. Oleschko, M. L. Juan, M. Silveri, and G. Kirchmair, *Nature Physics* **18**, 538 (2022).
- [51] D. Sels and A. Polkovnikov, *Proceedings of the National Academy of Sciences* **114**, E3909 (2017).
- [52] I. Čepaitė, A. Polkovnikov, A. J. Daley, and C. W. Duncan, *PRX Quantum* **4**, 010312 (2023).
- [53] T. Kato, *Journal of the Physical Society of Japan* **5**, 435 (1950).
- [54] J. A. Gyamfi, *European Journal of Physics* **41**, 063002 (2020).
- [55] A. S. Sheremet, M. I. Petrov, I. V. Iorsh, A. V. Poshakinskiy, and A. N. Poddubny, *Rev. Mod. Phys.* **95**, 015002 (2023).
- [56] D. Manzano and P. Hurtado, *Advances in Physics* **67**, 1 (2018).

Appendix A: Liouvillian gap analysis of timescale for $N = 2$

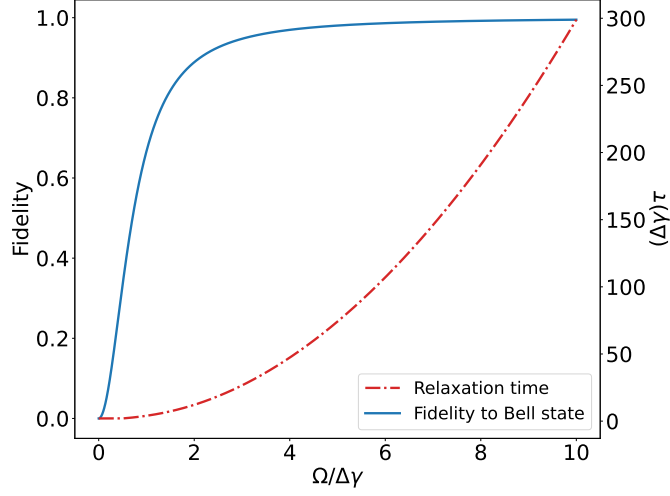


FIG. 4. Time taken to reach the steady state (left axis) and the fidelity F of the steady state to the dimer state (right axis) as a function of $\Omega/\Delta\gamma$.

Here, we perform a Liouvillian gap analysis for the case where $N = 2$ to supplement the result in the main text, which uses a different formalism [37] to prove that the timescale of forming a dimer pair diverges. Here, we assume that the phase accumulated by the excitation ϕ_{jk} as it travels between two system qubits is an integer multiple of 2π . In this case, the coherent interaction between the i th spin and the j th spin mediated by the 1D bath becomes $(H_C)_{jk} = (i\Delta\gamma/2)(\sigma_j^\dagger\sigma_k - \sigma_j\sigma_k^\dagger)$ where $\Delta\gamma = \gamma_R - \gamma_L$, and the collective decay into the 1D bath is given by $\Gamma\mathcal{D}[c]\rho$, where $\Gamma = \gamma_L + \gamma_R$ and $c = \sum_{i=1}^N \sigma_i$. In this section, we consider the case where the system qubits are driven using a time independent Hamiltonian $H_{\text{drive}} = (\Omega/2) \sum_{i=1}^N \sigma_i^x$, though the driving Hamiltonian could also be time dependent.

To obtain the steady state for this case, we solve

$$\dot{\rho} = -i[H_S + \sum_{j<k} (H_C)_{jk}, \rho] + \Gamma\mathcal{D}[c]\rho \quad (\text{A1a})$$

$$H_S = -\sum_{i=1}^N \delta_i \sigma_i^\dagger \sigma_i + H_{\text{drive}}(t) \quad (\text{A1b})$$

Eq. (A1) for $\rho_{ss} = 0$ with $N = 2$. One way to do this [54] is to vectorise the density matrix, i.e

$$\rho = \sum_{i,j} \rho_{ij} |i\rangle\langle j| \rightarrow |\rho\rangle = \frac{1}{C} \sum_{i,j} \rho_{ij} |i\rangle \otimes |j\rangle \quad (\text{A2a})$$

$$A\rho_S \rightarrow (A \otimes \mathbb{1})|\rho_S\rangle \quad (\text{A2b})$$

$$\rho_S B \rightarrow (\mathbb{1} \otimes B^T)|\rho_S\rangle \quad (\text{A2c})$$

where $|\rho\rangle$ is the vectorised form of ρ , which itself can be thought of as a ket in the so-called Liouville space [54], A and B are arbitrary operators, and B^T denotes the transpose of B . The constant C in $|\rho\rangle$ can be determined by normalising the state $|\rho\rangle$. With the above description, the master equation becomes

$$\frac{d|\rho\rangle}{dt} = L|\rho\rangle \quad (\text{A3})$$

where

$$L = -i(H \otimes \mathbb{1} - \mathbb{1} \otimes H^T) + \Gamma \left(c \otimes c^* - \frac{1}{2}(c^\dagger c \otimes \mathbb{1} - \mathbb{1} \otimes c^\dagger c) \right) \quad (\text{A4a})$$

$$H = \frac{-i\Delta\gamma}{2}(\sigma_2^\dagger \sigma_1 - \sigma_1 \sigma_2^\dagger) + \frac{\Omega}{2}(\sigma_1^x + \sigma_2^x) \quad (\text{A4b})$$

$$c = \sigma_1 + \sigma_2. \quad (\text{A4c})$$

We note that for $N = 2$, we can get a unique steady state even without imposing extra conditions on δ_i [26], and hence we have set all the $\delta_i = 0$. Then, solving for the steady state ρ_{ss} just reduces to finding the nullspace of the matrix L . In this case, we have a unique steady state

$$\rho_{ss} = |s\rangle\langle s| \quad (\text{A5a})$$

$$|s\rangle = \frac{1}{\sqrt{2 + (\frac{\Delta\gamma}{\Omega})^2}} \left(\frac{i\Delta\gamma}{\Omega} |gg\rangle - |ge\rangle + |eg\rangle \right). \quad (\text{A5b})$$

Clearly, in the $\Omega/\Delta\gamma \rightarrow \infty$ limit, we obtain the dimer state $|S\rangle = (|ge\rangle - |eg\rangle)/\sqrt{2}$ as the steady state of our system with fidelity 1.

From L , we can also calculate the (slowest) timescale for the system to relax to the steady state by calculating the inverse of the Liouvillian gap, which is the largest non-zero real part of the eigenvalues of the matrix L [56] (note that all the non-zero eigenvalues of L have negative real parts). For $\Omega \ll \Delta\gamma$, the Liouvillian gap is $-\Delta\gamma/2$, which means that the system relaxes to the steady state at a timescale $\tau = 2/\Delta\gamma$, independent of the driving strength. On the other hand, for $\Omega \gg \Delta\gamma$, the Liouvillian gap is $-\Delta\gamma^3/(3\Omega^2)$, which means that the system relaxes to the steady state at a timescale $\tau = 3\Omega^2/\Delta\gamma^3$. In Fig. 4, we plot both the fidelity of the steady state to the dimer state as well as the timescale τ (in units of $\Delta\gamma^{-1}$) required to reach that steady state as a function of $\Omega/\Delta\gamma$. In fact, we have

$$F = \frac{2\Delta\gamma\tau}{2\Delta\gamma\tau + 3}, \quad \Delta\gamma\tau = \frac{3}{2} \left(\frac{1}{1-F} - 1 \right) \quad (\text{A6})$$

where $F = \langle S|\rho_{ss}|S\rangle$ is the fidelity of the steady state to the dimer state. This means that $\Delta\gamma\tau = \mathcal{O}((1-F)^{-1})$ as $F \rightarrow 1$. In other words, the time required to obtain a dimer state as the steady state diverges with the required fidelity of the state preparation procedure. However, repeating the Liouvillian gap analysis for $N > 2$ qubits quickly becomes analytically intractable as N increases, which is why in the main text we used the formalism as described in [37] to prove the divergent timescale of obtaining the entangled steady state in general.

Appendix B: Derivation of the divergent timescale of preparing entangled dark states

For the system studied in the main text described by the master equation A1, it was shown [26] that with certain conditions on δ_i or in the chiral case $\gamma_L \neq \gamma_R$, it is possible to obtain the following multipartite entangled dark steady state for even N

$$\rho_{ss} = |\Phi\rangle\langle\Phi|, \quad \text{where } |\Phi\rangle = \prod_{q=1}^{N_m} |M_q\rangle \quad (\text{B1a})$$

$$\begin{aligned} |M_q\rangle = & a^{(0)} |g\rangle^{\otimes M_q} + \sum_{j_1 < j_2} a_{j_1, j_2}^{(1)} |S\rangle_{j_1 j_2} |g\rangle^{\otimes M_q - 2} \\ & + \cdots + \sum_{j_1, \dots, j_{M_q/2}} a_{j_1, \dots, j_{M_q/2}}^{(M_q/2)} |S\rangle_{j_1 j_2} \cdots |S\rangle_{j_{M_q-1} j_{M_q}}. \end{aligned} \quad (\text{B1b})$$

Here, we define $|S\rangle_{ij} = (|e\rangle_i |g\rangle_j - |g\rangle_j |e\rangle_i) / \sqrt{2}$ as a singlet state (or a dimer pair) between qubits i and j . $|\Phi\rangle$ is a product of N_m adjacent multimers $|M_q\rangle$, and each $|M_q\rangle$ is an entangled state over M_q qubits as defined in Eq. (B1b), where M_q is an even number. Note that the summation in the last line of Eq. (B1b) runs over all different pairings of qubits $\{(j_1, j_2), \dots, (j_{M_q-1}, j_{M_q})\}$ with $j_k < j_{k+1}$. It can also be shown that $a^{(i)} \propto |\Omega|^{-M_q/2+i}$.

Here, we want to use the general quantum speed limit framework for dissipative state preparation introduced in [37] to provide a lower bound for the time T required to generate the state in Eq. (B1) for any even system size N . From [37], we have

$$T \geq T_{\text{QSL}} \propto \frac{1}{\mathcal{A}} \quad (\text{B2})$$

where \mathcal{A} in our case is simply $|\Gamma| \times \|c^\dagger |\Phi\rangle\langle\Phi| c\|_F$ where $\|X\|_F \equiv \sqrt{\text{Tr}(X^\dagger X)}$ is the Frobenius norm of the operator X . Here, we recall that $c = \sum_{i=1}^N \sigma_i$. Now, from Eq. (B1b), we see that $c^\dagger |\Phi\rangle$ annihilates all kets in the linear combination except the ket $|g\rangle^{\otimes M_q}$. Thus, recalling that $a^{(0)} \propto |\Omega|^{-M_q/2}$, we have $\mathcal{A} = |\Gamma| \prod_{q=1}^{N_m} |\Omega|^{-M_q/2}$, which gives us

$$T \geq T_{\text{QSL}} \propto \prod_{q=1}^{N_m} |\Omega|^{M_q/2} = |\Omega|^{N/2} \sim \left(\frac{1}{1-F} \right)^{N/4}, \quad (\text{B3})$$

which diverges as $|\Omega| \rightarrow \infty$, or equivalently as the fidelity F to the target state in Eq. (D1) approaches unity. Crucially, for any fixed target fidelity F , the preparation time scales exponentially with the number of qubits N .

Appendix C: Comparison between our scheme and counterdiabatic driving

In the counterdiabatic driving scheme [38, 39], one often implements an extra time-dependent Hamiltonian $H_{\text{tqd}}(t)$ to speed up the adiabatic evolution due to a time-dependent Hamiltonian $H(t)$. Here, H_{tqd} cancels out the term in $H(t)$ that leads to transitions between different instantaneous eigenstates, and hence the system stays in its instantaneous eigenstate at all times regardless of how large $\partial_t H(t)$ is. Determining the form of $H_{\text{tqd}}(t)$ is generally a difficult process, as one needs to know all the time-dependent eigenstates of $H(t)$. Furthermore, in open quantum systems, the concept of transitionless driving is also further complicated by the need to maintain that the open systems evolution is a completely positive, trace-preserving (CPTP) map between density matrices at different times which might require one to engineer time-dependent dissipators [39].

However, for the problem we are considering in our paper, in the case where $\Delta\gamma \neq 0$, it is actually possible to use the idea of counterdiabatic driving in decoherence free subspaces [40]. We shall illustrate what we mean with the $N = 2$ example. From Eq. (A5), for the case where $\Delta\gamma \neq 0$, we see that by assuming $\Omega(t)$ is a monotonically increasing function of t such that $\Omega(0) = 0$, then as we slowly increase t from 0 to ∞ , we move from the instantaneous eigenstate of $H(0)$ which is $|gg\rangle$ to the instantaneous eigenstate of $H(\infty)$ which is $|S\rangle$. This follows from the adiabatic theorem of quantum mechanics [53]. Furthermore, since the instantaneous eigenstate of $H(t)$ is annihilated by c for all times t , when we use the technique of counterdiabatic driving, we avoid the complications that follow from attempting to do counterdiabatic driving for open quantum systems and we just need to consider the unitary evolution case, as mentioned in [40]. We note here that this scheme requires chirality, since if $\Delta\gamma = 0$, then there would not be an adiabatic trajectory that connects $|gg\rangle$ and $|S\rangle$.

Having explained how one might use counterdiabatic driving to speed up the many-body entanglement generation as proposed in [21, 26, 27], we note that the key difference between our scheme and counterdiabatic driving is that, for all intermediate times t between $t = 0$ and $t \rightarrow \infty$, there is no need for our system state to be an instantaneous eigenstate of $H(t)$. This is reflected in how our scheme allows for arbitrary choices of the function $\theta(\Omega(t))$ that fulfil $\theta(\Omega(0)) = 0$ and $\theta(\Omega(t \rightarrow \infty)) = \pi/2$. One practical implication of that is that unlike counterdiabatic driving, we do not require chirality. Furthermore, since counterdiabatic driving prevents transitions between all instantaneous eigenstates of $H(t)$, the construction of H_{tqd} would require knowledge of all of the eigenstates of $H(t)$ for all times t . On the other hand, since our scheme is only interested in constructing a trajectory between $|g \dots g\rangle$ and $|S\rangle_{i_1 i_2} |S\rangle_{i_3 i_4} \dots |S\rangle_{i_{N-1} i_N}$, we do not need to know all of the instantaneous eigenstates of $H(t)$.

To give a concrete example, we perform a comparison between our scheme and the counterdiabatic scheme for the $N = 2$ case. For the counterdiabatic driving scheme, we use $\gamma_R = 1, \gamma_L = 0$ which gives us $\Delta\gamma = 1$ and $\Gamma = 1$, whereas for our scheme, we use $\gamma_R = 0.5, \gamma_L = 0.5$ which gives us $\Delta\gamma = 0$ and $\Gamma = 1$. For our scheme, we also use

$$\theta(\Omega(t)) = \frac{\pi}{2}(1 - e^{-k\Omega(t)/\Gamma}), \quad k > 0, \quad (\text{C1})$$

Eq. (C1) with $k = 10$ for $\theta(\Omega(t))$. In both cases, we use $\Omega(t) = mt$ with the same value of m , and after $\Gamma t = 1$, we switch off the extra control field and we stop increasing the driving strength. For this case, we have:

$$\begin{aligned} H_{\text{tqd}}(t) = & \frac{1}{2} \frac{m}{1 + 2m^2 t^2} (\sigma_1^x - \sigma_2^x + \sigma_1^x \sigma_2^z - \sigma_1^z \sigma_2^x) + \frac{1}{2} \frac{2m^2 t}{1 + 6m^2 t^2 + 8m^4 t^4} (\sigma_1^x \sigma_2^y + \sigma_1^y \sigma_2^x) \\ & + \frac{1}{2} \frac{m}{1 + 6m^2 t^2 + 8m^4 t^4} (-\sigma_1^x + \sigma_2^x + \sigma_1^x \sigma_2^z - \sigma_1^z \sigma_2^x) \end{aligned} \quad (\text{C2a})$$

whereas for our scheme, we have $H_{\text{extra}}(t)$ as given in

$$H_{\text{extra}}(t) \approx \sum_{k \text{ odd}} V_{k,k+1} \quad (\text{C3a})$$

$$V_{k,k+1} = (\partial_t \theta) \left(\frac{1}{2} (\sigma_k^x - \sigma_{k+1}^x) + \frac{1}{2} (\sigma_k^x \sigma_{k+1}^z - \sigma_k^z \sigma_{k+1}^x) \right). \quad (\text{C3b})$$

Eq. (C3a). Notice that $H_{\text{extra}}(t)$ is simpler than $H_{\text{tqd}}(t)$ to implement experimentally as it has lesser many-body interaction terms. The simulation results are given in Fig. 5. Notice that after $t = 1$, since the counterdiabatic driving case requires us to stay in the instantaneous eigenstate of $H(t)$ given by Eq. (A5), the largest concurrence we can get is

$$C = \frac{2m^2 t^2}{1 + 2m^2 t^2} \quad (\text{C4})$$

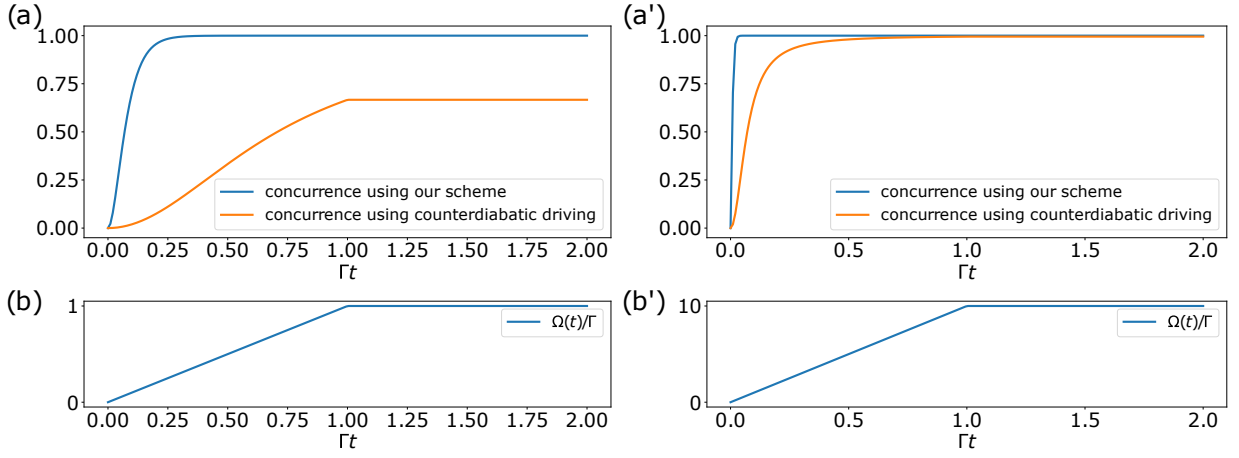


FIG. 5. In (a) and (a'), for the $N = 2$ case, we plot the concurrence of our scheme and the counterdiabatic driving scheme for $m = 1$ and $m = 10$ respectively, and in (b) and (b'), we show the time variation of the driving strengths $\Omega(t)$ against time. For our scheme, we use Eq. (C1) with $k = 10$ for $\theta(\Omega(t))$. Clearly, our scheme outperforms the counterdiabatic driving scheme, since we do not need to stay in the instantaneous eigenstate of $H(t)$ given in Eq. (A5).

which is the fidelity of Eq. (A5) to the dimer state $|S\rangle$. Hence as can be seen from Fig. 5, for the case where $m = 1$, we have a maximal concurrence of $2/3$ only. On the other hand, for our scheme, we can very quickly get concurrence 1 since we do not need to follow the adiabatic trajectory to get the final state $|S\rangle$.

Appendix D: Approximation of H_{extra}

In writing $H_{\text{extra}}(t) = H_u(t) - H_C - H_d(t) \approx H_u(t)$ in the main text, we made two approximations, first by ignoring $-H_C$ and next by ignoring $-H_d(t)$ in $H_{\text{extra}}(t)$. Here, we study the effect of both approximations. Here, we consider the problem of obtaining the state

$$|\Phi\rangle = \sum |S\rangle_{i_1 i_2} |S\rangle_{i_3 i_4} \cdots |S\rangle_{i_{N-1} i_N} \quad (\text{D1})$$

Eq. (D1) for general even N .

Effect of ignoring $-H_C$

Clearly, when $\Delta\gamma = 0$, ignoring $-H_C$ has no effect since $H_C = 0$. Hence, here we consider the case where $\Delta\gamma \neq 0$. For general even N , the steady state of Eq. (A1) is Eq. (B1), where as mentioned in the main text, we consider the case where we have only one multimer, i.e $N_m = 1$. For $|M_q\rangle$ in Eq. (B1), the coefficient in front of the $|g \dots g\rangle$ term is proportional to $\Delta\gamma^{N/2}$ for the case of zero detunings (i.e, $\delta_i = 0$ in Eq. (A1)).

Now, our scheme consists of switching on $H_{\text{extra}}(t)$ from $t = 0$ to $t = t_f$ where $t_f \equiv \Omega^{-1}(\theta^{-1}(\pi/2 - \epsilon))$ is as defined in the main text. After $t = t_f$, we switch off the extra driving field and keep the driving strength $\Omega(t)$ at a constant finite value $\Omega(t_f)$. As mentioned in the main text, this will give us a final state $|f\rangle$ that is $1 - \epsilon^2$ away in fidelity from Eq. (D1). At this point, since $\Delta\gamma \neq 0$ and since $\Omega(t)$ is finite, the state $|f\rangle$ is not an instantaneous eigenstate of $H(t)$. Hence, there will be transitions induced by $H(t)$ on $|f\rangle$ to all the instantaneous eigenstates of $H(t)$, some of which are not dark states. Hence, the state becomes mixed and the fidelity to Eq. (D1) drops. Note that depending on the choice of $\theta(t)$, since $|H_{\text{extra}}(t)| \propto \partial_t \theta$, if $\partial_t \theta \approx 0$ before t_f , then the above effect becomes more pronounced since we obtain the final state $|f\rangle$ before t_f . However, if $\Delta\gamma/\Omega(t)$ is small enough, then the probability amplitude of $|g \dots g\rangle$ component in the dark state given in Eq. (B1) will be small, which means that the overlap between the $|f\rangle$ and the dark state will be large. This means that the transitions induced by $H(t)$ on $|f\rangle$ will largely be to the dark state, which means that the fidelity to Eq. (D1) remains high.

We illustrate the above with the $N = 8$ case where we form 4 dimers, i.e where our target steady state is $|\Phi\rangle = |S\rangle_{12}|S\rangle_{34}|S\rangle_{56}|S\rangle_{78}$. For our scheme, we use $\gamma_R = 1, \gamma_L = 0$ which gives us $\Delta\gamma = 1$ and $\Gamma = 1$. Here, we consider $\Omega(t) = mt, m > 0$, and after $t = t_f = 1/\Gamma$, we switch off $H_{\text{extra}}(t)$ and fix $\Omega(t)$ at the constant value $\Omega(t_f)$. We also choose $\theta(\Omega(t))$ according to Eq. (C1) with $k = 10$. In Fig. 6 we show the extent of the negative effect that chirality has on our system at different values of $\Omega(t_f)$.

Effect of ignoring $-H_{\text{drive}}(t)$

Firstly, defining the triplet state $|T\rangle_{ij} \equiv (|e\rangle_i |g\rangle_j + |g\rangle_i |e\rangle_j)/\sqrt{2}$, the $H_{\text{drive}}(t)$ term can be written as $H_{\text{drive}}(t) = H'_{\text{drive}}(t) + O(t)$ where $H'_{\text{drive}}(t) = \frac{\Omega(t)}{\sqrt{2}} \sum (|T\rangle_{ij} \langle gg|_{i_1 i_2} + \cdots + |T\rangle_{ij} \langle gg|_{i_{N-1} i_N} + \text{H.c})$ and $O(t) = \Omega(t) \sum (|T\rangle_{ij} \langle ee|_{i_1 i_2} + \cdots + |T\rangle_{ij} \langle ee|_{i_{N-1} i_N} + \text{H.c})/\sqrt{2}$, and where the sum is over all pairs $\{(i_1, i_2), (i_3, i_4), \dots, (i_{N-1}, i_N)\}$ with $i_j < i_{j+1}$. In this decomposition, $O(t)$ annihilates the decoherence-free subspace, and since it commutes with $H_u(t)$, we can ignore the effect of $O(t)$. Hence, it remains to study the effect of ignoring $-H'_{\text{drive}}(t)$.

The idea is that if the transformation $|g \dots g\rangle \rightarrow |\Phi\rangle$ due to $H_u(t)$ is much quicker than the transformation $|g \dots g\rangle \rightarrow |T\rangle_{i_1 i_2} \cdots |T\rangle_{i_{N-1} i_N}$ due to $H'_{\text{drive}}(t)$, then the effect of ignoring $-H'_{\text{drive}}(t)$ is negligible. This can be done in many ways, for example by choosing $\theta(\Omega(t))$ according to Eq. (C1) with a large value of k . An example for the $N = 8$ case where we form 4 dimers, i.e where our target steady state is $|\Phi\rangle = |S\rangle_{12}|S\rangle_{34}|S\rangle_{56}|S\rangle_{78}$ is shown in Fig. 7 below. Since we studied the effect of a non-zero $\Delta\gamma$ above, here we set $\Delta\gamma = 0$ to solely study the effect of ignoring $H'_{\text{drive}}(t)$. As can be seen from Fig. 7, for small k such that the transformation $|g \dots g\rangle \rightarrow |\Phi\rangle$ is slow, the effect of ignoring $H'_{\text{drive}}(t)$ leads to quite substantial errors, but for large k , we can safely ignore $-H'_{\text{drive}}(t)$.

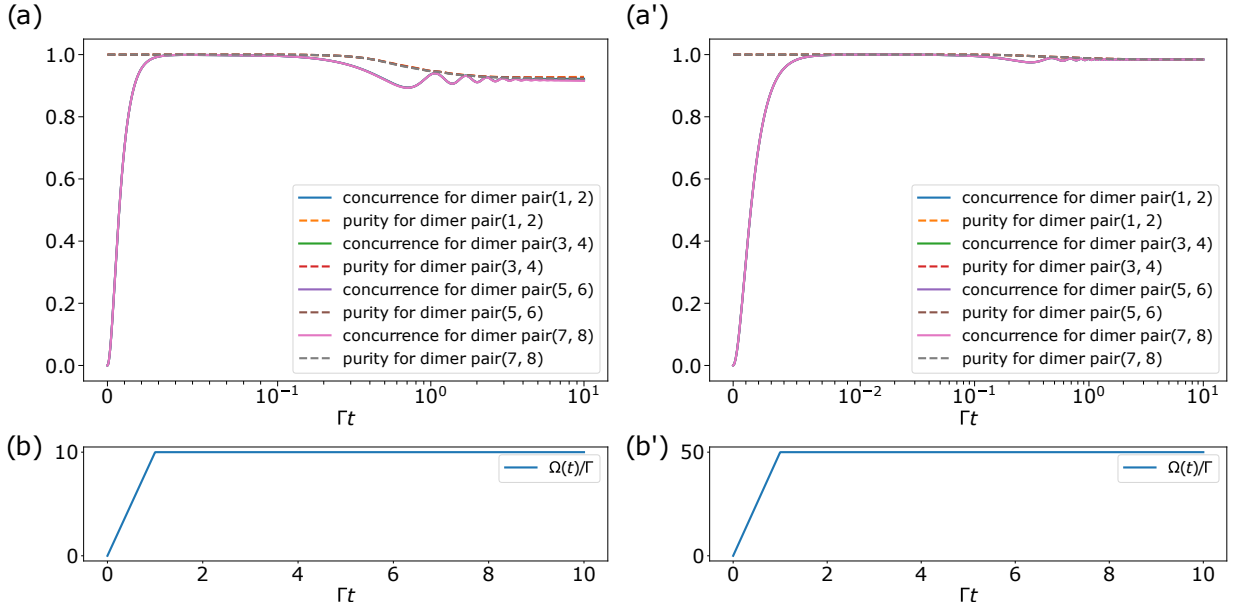


FIG. 6. Here, we study the effect of ignoring $-H_C$ in H_{extra} when $\Delta\gamma/\Gamma = 1$. In (a) and (a'), for the case where we have $N = 8$ qubits forming 4 dimer pairs, we plot both the concurrences of the dimer pairs as well as the purity of the dimer pairs for $m = 10$ and $m = 50$ respectively. In (b) and (b'), we plot the variation of the driving strength $\Omega(t)$ as a function of time. As can be seen, in both (a) and (a'), we quickly obtain the state $|\Phi\rangle$, even before we switch off $H_{\text{extra}}(t)$. This is because the form of Eq. (C1) with $k = 10$ causes $H_{\text{extra}}(t)$ to be very close to zero even before $\Gamma t = 1$. Then, in (a), since Ω is not high enough, the state $H(t)$ induces transitions on $|\Phi\rangle$ and together with the jump operators, we get a mixed state. In (a'), since Ω is high enough, the transitions induced by $H(t)$ are largely onto the dark state and hence the state largely remains pure.

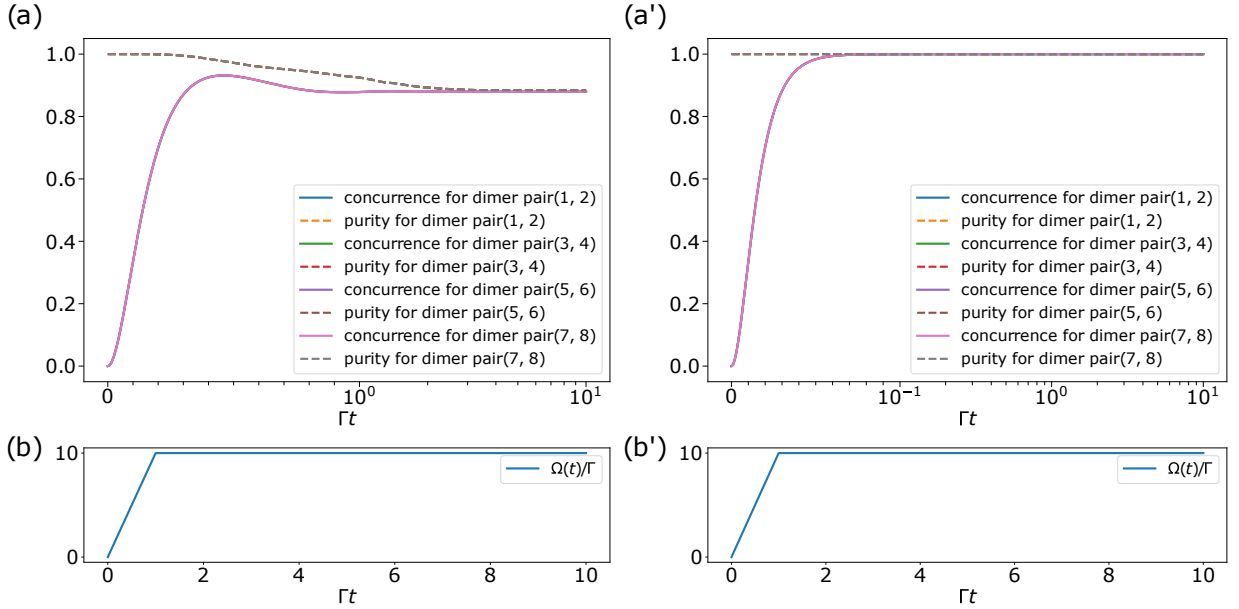


FIG. 7. Here, we study the effect of ignoring $-H'_{\text{drive}}$ in H_{extra} when $\Delta\gamma = 0$. In (a) and (a'), for the case where we have $N = 8$ qubits forming 4 dimers, we plot both the concurrences of the dimer pairs as well as the purity of the dimer pairs for $m = 10$. In (b) and (b'), we plot the time variation of the driving strength $\Omega(t)$. In both (a) and (a'), we use Eq. (C1) for $\theta(\Omega(t))$ with $k = 0.5$ and $k = 5$ respectively. Clearly, it is permissible to ignore $-H'_{\text{drive}}$ at large k . This is because the system goes from $|g \dots g\rangle$ so rapidly that $-H'_{\text{drive}}$ has no effect.

Appendix E: Effect of single spin spontaneous emission into free space on our scheme

Here, we consider the effect that single spin spontaneous emission on entanglement generation for both our scheme and the time-independent schemes in [21, 26, 27]. Single spin spontaneous emission into free space can be modelled by adding an additional term $\Gamma_f \sum_{i=1}^N \mathcal{D}[\sigma_i]\rho$ into Eq. (A1). The presence of Γ_f means that the pure state $|\Phi\rangle$ as defined in Eq. (B1) is no longer a steady state of the master equation dynamics. This leads to a reduction in the long-time purity as well as the amount of long-time entanglement generated for the time-independent schemes, as mentioned in [21, 26]. Our scheme also suffers a similar reduction in long-time purity as well as long-time entanglement generated, as our scheme is an accelerated form of the time-independent schemes.

However, we note that for waveguide QED systems, high β factors [55] of up to $\beta = 0.99$ have been experimentally demonstrated, where the β factor is defined as $\beta = \Gamma/(\Gamma + \Gamma_f)$, which is the ratio of the system radiative decay into the 1D bath over the total radiative decay rate of the system. Thus, in terms of the timescale defined by Γ^{-1} , Γ_f is largely negligible as long as Γ_f is small enough. Since our accelerated scheme is able to generate entanglement at time $\Gamma t \leq 1$, the maximal entanglement generated by our scheme remains high. Furthermore, the entanglement generated is still relatively long lived in terms of the timescale defined by Γ^{-1} . On the other hand, because the time-independent schemes require a long time for entanglement generation, the presence of Γ_f would affect the maximal entanglement that is generated.

To see the effects mentioned above, we consider the case of preparing $N/2$ local dimers from N qubits, i.e we want to prepare $|\Phi\rangle = |S\rangle_{1,2}|S\rangle_{3,4}\dots|S\rangle_{N-1,N}$. For the time-independent scheme, we consider the non-chiral case with the detuning pattern on the qubits $[\delta_1, -\delta_1, \delta_2, -\delta_2, \dots, \delta_{N/2}, -\delta_{N/2}]$ where $\delta_i \neq \delta_j$. This is the detuning pattern that leads to the formation of local dimer pairs with the time-independent scheme [26]. We will use the same parameters as the recent experimental work Ref. [28] where the authors implemented the time-independent scheme in [26]. This means that we use $\Omega/\Gamma \approx 5$ for the time-independent scheme with $\delta_i/\Omega \approx 1/2$ and $\Delta\gamma = 0$. On the other hand, for our time-dependent scheme, we use the same value of Ω/Γ but instead we use $\delta_i = 0$, since our scheme does not need the detunings to produce the local dimers. We will consider both $\Gamma_f/\Gamma = 0.1$ which is demonstrated in [28] for implementing the time-independent scheme and also $\Gamma_f/\Gamma = 0.01$ which is achievable with current experimental techniques for superconducting qubit platforms [50, 55].

Firstly, we show that for the above experimental parameters, the steady state concurrence C of each dimer pair and its fidelity to the Bell state F dips significantly below 1 even for small values of Γ_f for $N \geq 4$. This numerically demonstrates our claim above that in the steady state, both the time-independent scheme and our scheme are adversely affected by free-space decay. This is intuitively obvious from the fact that the steady state is the $t \rightarrow \infty$ state of the master equation dynamics, which means even a small amount of free-space decoherence Γ_f can have a large effect. A summary of results for C and F in the steady state is shown in Table I. We note that though larger values of δ_i can have a positive effect on entanglement generation (as measured by C), this effect becomes largely negligible as the number of system qubits N increases.

N, Γ_f	$\delta_i \approx \Omega/2$		$\delta_i \ll \Omega$	
	Steady state C	Steady state F	Steady state C	Steady state F
$N = 4, \Gamma_f = 0.01, 0.10$	0.137, 0.083	0.684, 0.667	0, 0	0.489, 0.486
$N = 6, \Gamma_f = 0.01, 0.10$	0.015, 0	0.650, 0.641	0, 0	0.489, 0.484
$N = 8, \Gamma_f = 0.01, 0.10$	0, 0	0.631, 0.626	0, 0	0.488, 0.480

TABLE I. Here we numerically solve for $\dot{\rho} = 0$ in Eq. (A1) with an additional dissipative term $\Gamma_f \sum_{i=1}^N \mathcal{D}[\sigma_i]\rho$ to find the steady state in the presence of free space spontaneous emission with rate Γ_f . Parameters used are: $\Delta\gamma = 0, \Omega/\Gamma = 5$, with the detuning pattern on the qubits given by $[\delta_1, -\delta_1, \delta_2, -\delta_2, \dots, \delta_{N/2}, -\delta_{N/2}]$ where $\delta_i = \Omega/2 + 0.01(i - 1)$ (in units of Γ) for the $\delta_i \approx \Omega/2$ case. We also consider the $\delta_i \ll \Omega$ case to study the effect that δ_i has on the steady state concurrence. For the $\delta_i \ll \Omega$ case, we have $\delta_i = 0.01i$ (in units of Γ). From the steady state obtained, we calculate fidelity F of the i th, i th + 1 qubit pair to the Bell state, as well as the concurrence C of the i th, i th + 1 spin pair. We then tabulate the average values of fidelity and concurrence across all qubit pairs. Note that with $\Gamma_f = 0$, we would expect $F, C \approx 1$ since the detuning pattern chosen as well as the high value of Ω/Γ would lead to the formation of perfect dimerised pairs [26].

Secondly, we show that as mentioned above, the high β factors in current experiments mean that even though the steady state has a low concurrence in the presence of Γ_f , we can still achieve reasonably long-lived entanglement (in units of the relevant timescale Γ^{-1}) if the entanglement can be generated fast enough. This would be possible with our scheme, but not with the time-independent schemes which take prohibitively long to generate the entanglement. More precisely, we note that the time-independent scheme fails when the preparation time required exceeds $\sim 1/\Gamma_f$, which

means that from Eq. (B3), we can estimate that the time-independent scheme to fail for $N \gtrsim \log(\Gamma/\Gamma_f)$. Examples for $N = 4, 6, 8$ are shown in Fig. 8. As can be seen, our scheme is able to achieve a high maximal concurrence of 1 for each dimer pair. Furthermore, the entanglement generated by our scheme is relatively long-lived. This is because our entanglement generation scheme is rapid and hence perfect quantum dimer pairs are formed before the spontaneous emission has any appreciable effect on our system. On the other hand, we see that the time-independent scheme fails to generate any substantial level of concurrence before the effect of spontaneous emission causes the concurrence to drop back to near zero. We note here that as shown in Table I, the large δ_i in the time-independent scheme allows for a small non-zero concurrence in the steady state in the $N = 4$ case. However, as can be seen, the effect of the large δ_i on the steady state concurrence becomes negligible for $N \geq 6$. We show the maximal concurrence generated by both our scheme and the time-independent scheme in Table II.

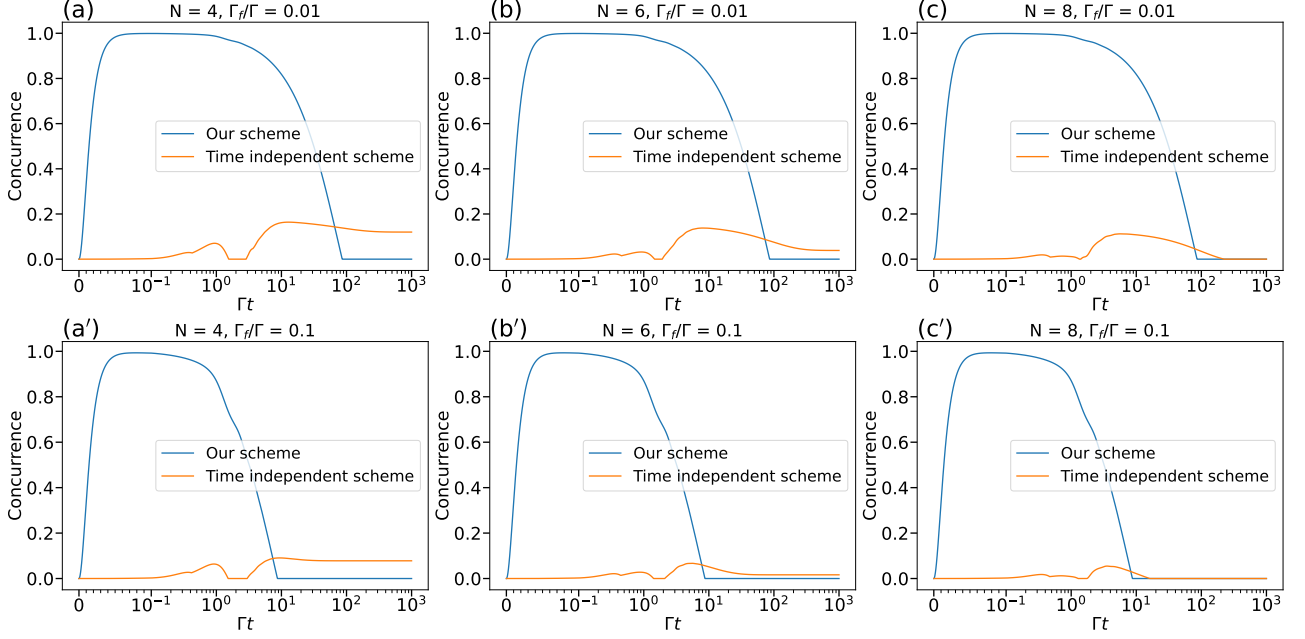


FIG. 8. Numerical experiments for the concurrence against time for both the time-independent scheme and for our scheme. Here, we use the same experimental parameters as in Table I. Plots (a), (b), (c) are for $N = 4, 6, 8$ qubits respectively, with $\Gamma_f/\Gamma = 0.01$. Plots (a'), (b'), (c') are also for $N = 4, 6, 8$ qubits respectively, but with $\Gamma_f/\Gamma = 0.1$. At long times Γt , the concurrence of both our scheme and the time-independent scheme drops to near-zero, in agreement with Table I. However, since our scheme is rapid, the entanglement is generated rapidly at $\Gamma t \ll 1$ before the effects of spontaneous emission kicks in, which allows our scheme to achieve a maximal concurrence of 1. Furthermore, the entanglement generated by our scheme is relatively long-lived in units of Γ^{-1} , especially for smaller values of Γ_f . Thus, our scheme achieves a high maximal concurrence of 1. On the other hand, the time-independent scheme generates entanglement too slowly and the effect of spontaneous emission kicks in even before any appreciable entanglement is generated, as can be seen by the concurrence dipping to near-zero at long times.

N, Γ_f	Maximal concurrence reached by our scheme	Maximal concurrence reached by the time-independent scheme
$N = 4, \Gamma_f = 0.01, 0.10$	1, 1	0.163, 0.091
$N = 6, \Gamma_f = 0.01, 0.10$	1, 1	0.137, 0.067
$N = 8, \Gamma_f = 0.01, 0.10$	1, 1	0.112, 0.055

TABLE II. Maximal concurrence generated by both our scheme and by the time-independent scheme, using the same experimental parameters as per Table I. Clearly, only our scheme achieves a high maximal concurrence.

Appendix F: Effect of unequal local light-matter coupling

The effect of unequal local light-matter coupling in our system is captured by the term $\sum_{i=1}^N \delta_i \sigma_i^\dagger$ in Eq. (A1) in the form of different detunings of the spins to the driving field H_{drive} . To obtain dimerised pairs in the steady state in the case of time-independent driving, it is required that the detunings on the spins follow a specific pattern

$$[\delta_1, -\delta_1, \delta_2, -\delta_2, \dots, \delta_{N/2-1}, -\delta_{N/2}] \quad (\text{F1})$$

where $\delta_i \neq \delta_j$, for the case where $N > 2$ [26]. On the other hand, for our protocol with time-dependent driving, we actually do not require engineering such a detuning pattern on the qubits, i.e our protocol works even with $\delta_i = 0$ for all qubits. In this section, we study the effect of $\delta_i \neq 0$ for our protocol, which may be a result of experimental imprecision in the creation of the qubits.

When $\delta_i \neq 0$ but δ_i still obeys the detuning pattern as per Eq. (F1), our protocol would still produce dimerised pairs in the steady state. In this case, the concurrence of the dimerised pairs would depend on the ratio $\Omega(t_f)/\max(\delta_i)$ where we recall that t_f is the time after which the strength of the driving field $\Omega(t)$ remains constant. This is because while the detuning pattern in Eq. (F1) guarantees the formation of dimerised pairs as per [26], the singlet fraction of each dimer pair depends on the relative strength of Ω as compared to the other parameters in the system. Since the detuning pattern obeys Eq. (F1), we note that after a sufficiently long time (see Appendix B for the lower bound on the time taken), the time independent scheme would also produce the state of dimerised pairs. A numerical example comparing our scheme to the time-independent scheme in this case is shown in Figure 9a. In the event that $\delta_i \neq 0$

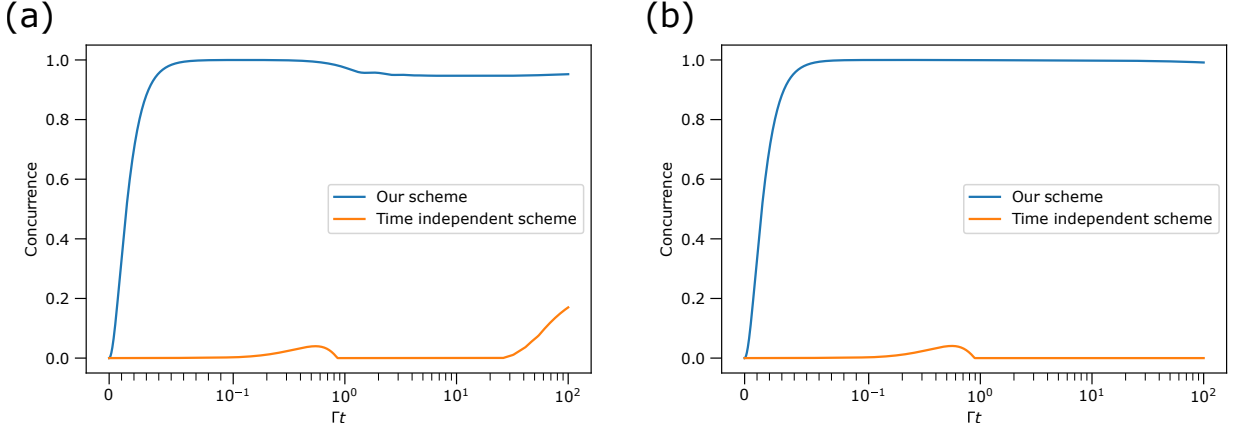


FIG. 9. In (a) and (b) respectively, we plot the effect of detunings on the average concurrence when $N = 8$ qubits form $N/2 = 4$ dimer pairs for the cases when the detunings on each qubit obey Eq. (F1) and when the detunings on each qubit do not obey Eq. (F1). In (a), we see our scheme quickly reaches a high value of concurrence that decays to its true steady state value, which is lesser than 1 because of the detuning. On the other hand, the time independent scheme sees a rise in concurrence only after a long time. This shows that when Eq. (F1) is satisfied for the detuning patterns, both our scheme and the time independent scheme can generate dimerised pairs in the steady state, though our scheme accelerates the approach to this steady state. In (b), we see that while a violation of Eq. (F1) means that we will not get dimerised pairs in the steady state, our scheme is able to rapidly produce long-lived concurrence that decays quite slowly for the values of δ_i considered. On the other hand, the time-independent scheme fails to produce any meaningful amount of concurrence. The numerical parameters chosen are: $\Omega_{\text{max}}/\Gamma = 5$, $\delta_i/\Gamma = \{0.25, -0.25, 0.275, -0.275, 0.3, -0.3, 0.325, -0.325\}$ for (a) and $\delta_i/\Gamma = \{0.300, 0.296, 0.426, 0.405, 0.381, 0.459, 0.292, 0.429\}$ for (b), $\Delta\gamma = 0$. We also use Eq. (C1) in our scheme, with $k = 10$. Lastly, for our scheme, we set $\Omega(t)$ to increase linearly from 0 to its max value Ω_{max} after $\Gamma t = 1$, after which it will stay constant.

and that δ_i does not obey the detuning pattern in Eq. (F1), then the state of dimerised pairs will not be the steady state of the system. Thus, while our protocol can still produce the state of dimerised pairs, the i th dimerised pair decays with a rate proportional to δ_i/Ω . On the other hand, since δ_i does not follow the detuning pattern in Eq. (F1), the time independent scheme will not produce the state of dimerised pairs regardless of how long one waits, since the dimerised pair state will not be the steady state of the system. Since it is generally experimentally easier to set up detuning patterns δ_i that will not obey Eq. (F1), the fact that our scheme works in this case but the time independent scheme does not is noteworthy. A numerical example comparing our scheme to the time-independent scheme in this case is shown in Figure 9.

Appendix G: $N = 6$ multimers

First, we show numerically that our scheme works for a $N = 6$ multimer, i.e when our target state is

$$|\Phi\rangle = \sum |S\rangle_{i_1, i_2} |S\rangle_{i_3, i_4} |S\rangle_{i_5, i_6} \quad (\text{G1})$$

where the summation is over all possible pairs $\{(i_1, i_2), (i_3, i_4), (i_5, i_6)\}$ where $i_k < i_{k+1}$. By counting, we see that for N spins, we would have $(N-1)(N-3)\dots 1$ terms in the summation. Hence, for $N = 6$, this gives us 15 terms in our summation. Using $\Omega(t) = mt, m > 0$ and Eq. (C1) for $\theta(\Omega(t))$, in the case where $\Delta\gamma = 0$, a straightforward application of our scheme gives us the results in Fig. 10. Clearly, we are able to easily obtain the state $|\Phi\rangle$ numerically, and we are able to do so in $\Gamma t \ll 1$. However, for this case, the X operator is a linear combination of multiple many-body interaction terms, which means that experimental implementation of this scheme is still quite tricky with the current state of quantum control.

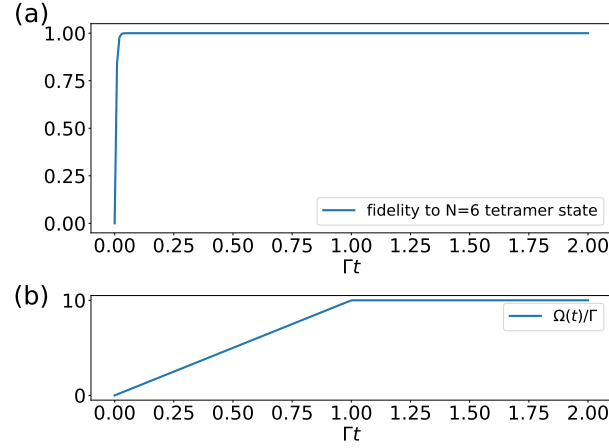


FIG. 10. In (a), we plot the fidelity of the system state to $|\Phi\rangle$, and in (b), we plot the time variation of the driving strength $\Omega(t)$. The numerical results here show that at least in theory, our scheme works.